AIP | Applied Physics Letters

Organic heterojunction photodiodes exhibiting low voltage, imaging-speed photocurrent gain

William T. Hammond and Jiangeng Xue

Citation: Applied Physics Letters **97**, 073302 (2010); doi: 10.1063/1.3481407
View online: http://dx.doi.org/10.1063/1.3481407
View Table of Contents: http://scitation.aip.org/content/aip/journal/apl/97/7?ver=pdfcov
Published by the AIP Publishing

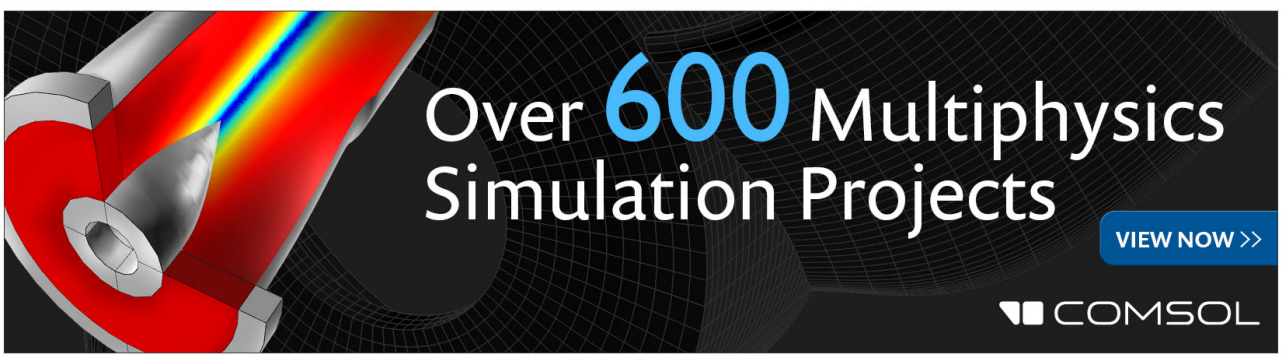

Organic heterojunction photodiodes exhibiting low voltage, imaging-speed photocurrent gain

William T. Hammond and Jiangeng Xue[a)]
Department of Materials Science and Engineering, University of Florida, Gainesville, Florida 32611, USA

(Received 30 March 2010; accepted 2 August 2010; published online 18 August 2010)

We report the demonstration of fast and strong photocurrent gain in organic photodiodes with tailored charge blocking layers. The hole blocking layer between the anode and the photoactive layer leads to accumulation of photogenerated holes at its interface with the active layer, which causes a strong secondary electron injection from the anode and as such a high photocurrent gain. Using a bulk heterojunction of C_{60} and copper phthalocyanine as the active layer, we have achieved photocurrent gains up to 500 across the visible spectrum and bandwidths on the order of 1 kHz, well above the imaging-compatible bandwidth (>60 Hz). © *2010 American Institute of Physics*. [doi:10.1063/1.3481407]

Organic photodiodes are regarded as a promising technology for a host of general photonic applications, due to the simple fabrication methods and high absorption coefficients across a broad spectral range spanning from ultraviolet through visible and near infrared, all of which are characteristic of organic semiconductors.[1] In fact, their promise has recently come to fruition with researchers achieving visible specific detectivity, D^*, similar to silicon photodiodes in both organic and organic-inorganic hybrid devices.[2,3] Furthermore, there is a growing body of work that demonstrates photoconductive gains in organic-based photodetectors,[4–9] which may make this technology suitable for applications in which low signals require amplification.

Photoconductive gain arises in devices that exhibit unbalanced carrier transport, such that minority photogenerated carriers are extracted or recombine on a longer time scale than the transit time of secondary majority photocurrent. Intrinsic carrier imbalance can lead to photocurrent gain in some materials, and in fact bulk photoconductive gain has been demonstrated in many organic devices.[4–6] Yet, it is also possible to engineer carrier imbalance into a device by introducing extrinsic trapping sites. For instance, Chen *et al.*[7] dispersed inorganic nanostructures as trapping centers into polymer-based photodetectors to achieve gain, and Yokoyama and colleagues attributed high gain in their small molecule-based devices to structural voids that trap holes at injection interfaces.[8,9]

Here, we report a general organic photodiode device architecture that employs heterojunctions formed by a vacuum-deposited, multilayer stack of small molecular weight organic materials. While gain in organic photodetectors generally has been relying on deep trap states within the organic layers and at interfaces, here we leverage the concept of carrier confinement by using blocking layers to simultaneously achieve strong and relatively fast photocurrent gain. Organic heterojunctions have been widely used in organic light-emitting devices, where various transport and confinement layers with desired energy levels have been employed to control the dynamics of charge carriers and excitons (bound electron-hole pairs) to achieve optimal performance.[10,11] Multilayer organic stacks have also been used in organic photodiodes, which were shown to strongly influence the dark current and photoresponse.[12–14] The charge blocking layers used here enable the confinement of holes at an interface, and by extension the realization of photoconductive gain, without the use of deep trap states with long lifetimes, leading to improved response time.

Organic heterojunction photodiodes were fabricated onto glass substrates with commercially coated indium-tin oxide (ITO) anodes (sheet resistance ≈15 Ω/square), prepared by successive sonication in detergent, deionized water, acetone, and isopropanol. A vacuum thermal evaporator with a base pressure of 10^{-7} Torr was used to successively deposit a dual hole blocking layer (HBL) consisting of a 2–3 nm thick naphthalenetetracarboxylic dianhydride (NTCDA) and a 10 nm thick C_{60} layer, a 50 nm thick mixed donor-acceptor heterojunction[14,15] of 70% (by weight) C_{60} (acceptor) and 30% copper phthalocyanine (CuPc) (donor), an 8 nm thick bathocuproine (BCP) exciton-blocking layer,[14] an 80 nm thick Al cathode, and a 200 nm thick MoO_3 encapsulation layer. C_{60}, CuPc, and BCP were purchased from MER Corp., Sigma Aldrich, and Tokyo Chemical Industry, respectively, while 99.999% Al and 99% MoO_3 were purchased from Alfa Aesar. C_{60} and CuPc were purified once by thermal gradient sublimation,[16] NTCDA was purified twice, and all other materials were used as received. A cross-bar geometry was used for the electrodes, defining an active device area of 0.04 cm^2.

Figure 1 shows the schematic energy level diagrams of our photodiode device structure under open-circuit condition (a) and under reverse bias with light illumination (b). In Fig. 1(a), the highest occupied and lowest occupied molecular orbital (HOMO and LUMO, respectively) energies, as well as the Fermi levels of the electrodes, are given in electronvolt as referenced from the vacuum level. Note that these values are approximate, as they are taken from photoelectron spectroscopic measurements[17,18] for individual layers without consideration of possible dipoles at interfaces. Our design requires a blocking layer to impose an energy barrier to the extraction of holes under a reverse bias, combined with a LUMO energy that does not introduce an additional electron injection barrier from the anode into the active layer. For the active layer, we use the CuPc–C_{60} donor-acceptor

a)Electronic mail: jxue@mse.ufl.edu.

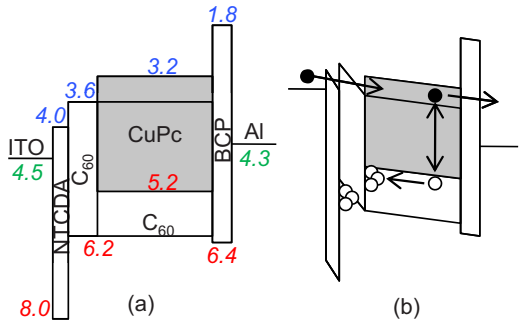

FIG. 1. (Color online) (a) Schematic energy level diagram of device under open circuit showing alignment of transport energy levels. The energies for the Fermi levels of the electrodes (ITO, Al) and the highest occupied (lower numbers) and lowest unoccupied (upper numbers) molecular orbitals of the organic materials are all referenced from the vacuum level in electronvolt. (b) Schematic energy level diagram of the illuminated device under reverse bias.

system[14,15] here as it has been widely studied for organic photovoltaic applications but other active layers could also be used to cover other spectral regions (such as near infrared). Photon absorption and subsequent exciton dissociation in the CuPc–C_{60} active layer lead to holes in the CuPc HOMO and electrons in the C_{60} LUMO level.[14,15] For holes in CuPc, NTCDA works well as a HBL, and C_{60} itself can also be used to block holes due to the ~1 eV HOMO level offset between CuPc and C_{60}.

The current density-voltage (*J-V*) characteristics of the device in the dark are shown in Fig. 2(a). The device exhibits diode characteristics with a rectification ratio of approximately 5×10^3 at ±1 V, although the reverse bias current increases strongly as the bias becomes more negative. It is believed that the dark current is dominated by electron injection/transport due to the very large hole injection barriers from either contact based on the energy level diagram shown in Fig. 1(a). Under reverse bias, electrons should experience significant barrier heights (~0.5 eV at the ITO/NTCDA interface and ~0.4 eV at the NTCDA/C_{60} interface) to inject from the ITO anode into the organic active layer, which limits the magnitude of the reverse-bias current. Under forward bias, however, it has been shown from CuPc:C_{60} based organic photovoltaic cells that there are negligible barriers for electron transport across the C_{60}/BCP/Al contacts.[14,15]

When the device is illuminated, photon absorption by either CuPc or C_{60} molecules in the active layer creates excitons that quickly dissociate at the CuPc–C_{60} interface, generating electrons on the C_{60} LUMO level and holes on the CuPc HOMO level.[15] As Fig. 1(b) depicts, when a reverse bias is applied, holes are swept toward the anode but accumulate at the interface between the active layer and the HBL due to the HOMO level offsets at the interfaces, whereas electrons are swept toward and collected at the cathode (the BCP layer does not impede electron transport as its energy levels apparently indicate due to formation of defect states in the energy gap upon Al deposition[14]). The accumulation of holes creates a large electric field across the HBL leading to increased injection of *secondary* electrons into the organic layers from the ITO anode due to thermionic-field emission or thermally assisted tunneling.[19] This mechanism follows the photoconductive gain model, in which the gain scales

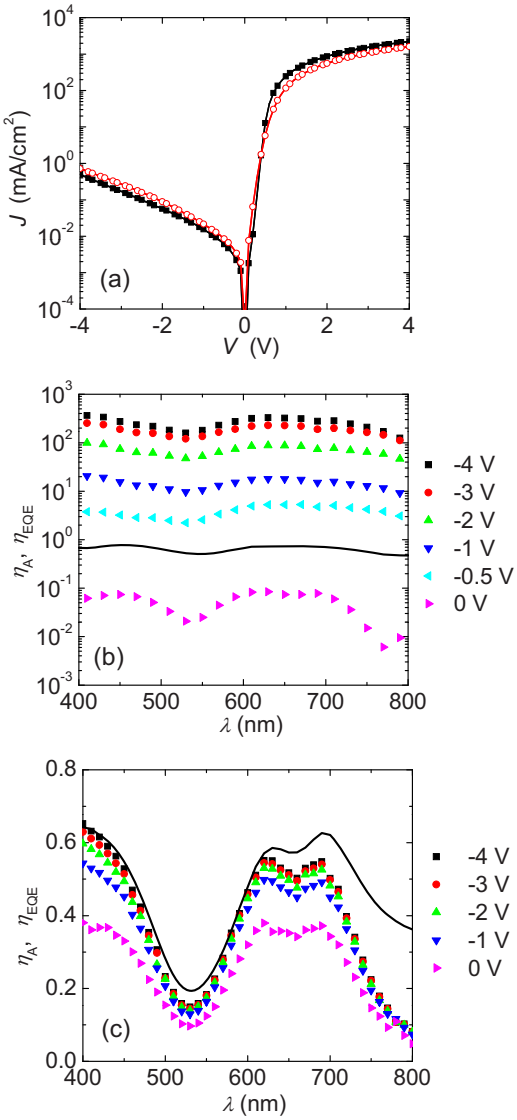

FIG. 2. (Color online) (a) Current density-voltage (*J-V*) characteristics in the dark for a CuPc:C_{60} organic heterojunction photodiode with a dual NTCDA/C_{60} blocking layer (open circles) and for a control device with no HBL but an otherwise identical structure (filled squares); (b) light absorption efficiency (η_A, solid line) and external quantum efficiency (η_{EQE}, symbols) as a function of the wavelength (λ) at several applied voltages for the device with the HBL; and (c) η_A (solid line) and η_{EQE} (symbols) for the control device without the HBL.

with the ratio of the lifetime of the confined holes to the secondary electron transit time through the device.

Indeed, we find that this device structure realizes high gain with low applied biases. Figure 2(b) shows the external quantum efficiency (η_{EQE}) as a function of the incident monochromatic light wavelength (λ) at various applied biases. Devices were illuminated by monochromatic light from λ=400 to 800 nm (with an average intensity of 40 $\mu W/cm^2$) modulated at 25 Hz by an optical chopper and photocurrent was measured using a Keithley 428 current amplifier and Stanford Research 540 lock-in amplifier. As shown in Fig. 2(b), $\eta_{EQE}>1$ across the entire wavelength range of interest is achieved at $V=-0.5$ V, suggesting the existence of a gain mechanism. A further increase in the reverse bias leads to a drastic increase in η_{EQE}, reaching a maximum of 90 at $V=-2$ V and 340 at −4 V in the red portion of the spectrum where CuPc absorbs strongly. Con-

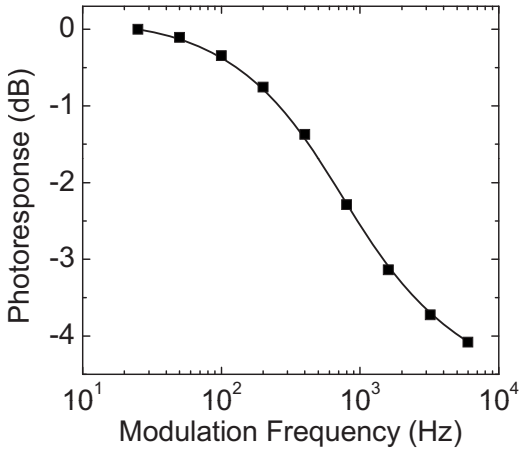

FIG. 3. Photocurrent response of the organic photodiode with the HBL at an applied bias of $V=-3$ V as a function of the frequency of the modulated optical excitation, normalized to the response measured at 25 Hz.

sidering that the total light absorption efficiency of the device [solid line in Fig. 2(b)] is $\eta_A \approx 65\%$ in this range, this device achieves a maximum gain ($G=\eta_{EQE}/\eta_A$) of approximately 500 at $V=-4$ V. We also found that either the NTCDA or C_{60} HBL works on its own to produce maximum photocurrent gains of 10–30 in this device structure; however, the use of both HBLs achieves the highest gains as described above.

To confirm the origin of the observed gain, we have also fabricated a control device without the HBL, but with an otherwise identical active layer structure. The dark J-V characteristics of this control device are very similar to those for the device with the HBL as shown in Fig. 2(a). As shown in Fig. 2(c), under zero bias (or short-circuit), η_{EQE} of the control device is about three times higher than that of the device with the HBL [see Fig. 2(b)], due to more efficient hole extraction. However, with increasing reverse bias, η_{EQE} of the control device saturates below unity, approaching η_A of the device [solid line in Fig. 2(c)]. The drastically different photoresponsive characteristics of the two devices under reverse bias clearly confirm that the observed gain in devices with the HBL is indeed related to the function of the HBL rather than to the bulk properties of the active layer.

We have also characterized the frequency response of the device by varying the optical chopper modulation frequency from 25 Hz to 6 kHz, keeping an applied bias of $V=-3$ V. Figure 3(a) shows the magnitude of the photocurrent at a wavelength of $\lambda=690$ nm normalized to that measured at 25 Hz as a function of the chopping frequency. Under these conditions, the organic heterojunction photodiode achieves a 3 dB frequency of $f_{3dB} \approx 1$ kHz and a gain-bandwidth product of 2×10^5 at $V=-3$ V. This bandwidth is remarkable for an organic photodiode exhibiting a strong gain mechanism, as these properties have appeared mutually exclusive in prior art devices.[4,8,9] We believe that the manner in which the HBL accumulates holes within the device is responsible for the relatively fast photoresponse. While in previously reported devices holes are trapped in localized states, the device reported here confines holes at the active layer/HBL interface at which they still have the ability to freely move within the plane. The bulk of the photoactive layer does not provide trapping sites to promote intrinsic photocurrent gain as shown by the lack of gain in control devices without the HBL (the hole mobility in the CuPc:C_{60} mixed layer with 30% CuPc is on the order of $10^{-6}-10^{-5}$ $cm^2/V\,s$ at an electric field of $\sim 5\times10^5$ V/cm).[20] Therefore, when light is no longer incident on the device, confined holes recombine via bimolecular recombination with injected electrons until the dark diode behavior is reclaimed, without the long release time of trap-based devices.

In summary, we have introduced a new organic photodiode device structure that achieves both high gain and relatively high operation speed under low applied bias. The photocurrent gain mechanism is attributed to the interfacial confinement of photogenerated holes due to the barrier height presented by the tailored HBLs. Under an applied bias of only $V=-3$ V, our device achieves a gain-bandwidth product of 2×10^5, the highest reported value for an organic-based device under such low applied voltage. Furthermore, such a device can be operated at a frequency well above 60 Hz, a typical imaging refresh rate. We propose that this device structure may be useful for imaging applications, especially those that require large area detection of low signals that require amplification.

Partial financial support to this work was provided by the National Science Foundation CAREER Program (ECCS 0644690).

[1] S. R. Forrest, Nature (London) **428**, 911 (2004).
[2] M. Ramuz, L. Bürgi, C. Winnewisser, and P. Seitz, Org. Electron. **9**, 369 (2008).
[3] X. Gong, M. Tong, Y. Xia, W. Cai, J. S. Moon, Y. Cao, G. Yu, C.-L. Shieh, B. Nilsson, and A. J. Heeger, Science **325**, 1665 (2009).
[4] I. H. Campbell and B. K. Crone, Appl. Phys. Lett. **95**, 263302 (2009).
[5] J. Gao and F. A. Hegmann, Appl. Phys. Lett. **93**, 223306 (2008).
[6] J. Reynaert, V. I. Arkhipov, P. Heremans, and J. Poortmans, Adv. Funct. Mater. **16**, 784 (2006).
[7] H.-Y. Chen, L. K. F. G. Yang, H. G. Monbouquette, and Y. Yang, Nat. Nanotechnol. **3**, 543 (2008).
[8] M. Hiramoto, K. Nakayama, I. Sato, H. Kumaoka, and M. Yokoyama, Thin Solid Films **331**, 71 (1998).
[9] G. Matsunobu, Y. Oishi, M. Yokoyama, and M. Hiramoto, Appl. Phys. Lett. **81**, 1321 (2002).
[10] Y. Zheng, S.-H. Eom, N. Chopra, J. Lee, F. So, and J. Xue, Appl. Phys. Lett. **92**, 223301 (2008).
[11] S.-H. Eom, Y. Zheng, E. Wrzesniewski, J. Lee, N. Chopra, F. So, and J. Xue, Org. Electron. **10**, 686 (2009).
[12] J. Xue and S. R. Forrest, J. Appl. Phys. **95**, 1859 (2004).
[13] J. Xue and S. R. Forrest, J. Appl. Phys. **95**, 1869 (2004).
[14] P. Peumans, A. Yakimov, and S. R. Forrest, J. Appl. Phys. **93**, 3693 (2003).
[15] S. Uchida, J. Xue, B. P. Rand, and S. R. Forrest, Appl. Phys. Lett. **84**, 4218 (2004).
[16] S. R. Forrest, Chem. Rev. (Washington, D.C.) **97**, 1793 (1997).
[17] B. P. Rand, D. P. Burk, and S. R. Forrest, Phys. Rev. B **75**, 115327 (2007).
[18] A. Kahn, N. Koch, and W. Gao, J. Polym. Sci., Part B: Polym. Phys. **41**, 2529 (2003).
[19] K. C. Kao and W. Hwang, *Electrical Transport in Solids* (Pergamon, New York, 1981).
[20] B. P. Rand, J. Xue, S. Uchida, and S. R. Forrest, J. Appl. Phys. **98**, 124902 (2005).